ENHANCED BUCK CONVERTER WITH UNIVERSAL MODEL FOR THE SWITCHED VOLTAGE REGULATORS

Dobroslav Kováč*, Irena Kováčová

Department of Theoretical and Industrial Electrical Engineering, Faculty of Electrical Engineering and Informatics, Technical University of Kosice, Kosice, Slovak Republic

*E-mail of corresponding author: dobroslav.kovac@tuke.sk

Dobroslav Kováč 0000-0002-9930-9272, Irena Kováčová 0000-0003-0482-6646

Resume

This article presents the enhancement and refinement of a simulation model for an integrated universal switched voltage regulator compatible with PSPICE software. The model enables users to create representations of any specific type of switched voltage regulator currently available on the market. The described regulator model is practically applied in widely used configurations of buck converters, including applications in transportation. The accuracy of the regulator model is verified by comparing the simulated waveforms of the converter to those provided in its datasheet. Additionally, the model is employed for the design and simulation analysis of buck converter circuits, with extended current and voltage ranges for their output parameters. In the context of improving the performance of such converters, particular attention is given to enhancing their electromagnetic compatibility.

Article info

Received 29 January 2025
Accepted 25 February 2025
Online 12 March 2025

Keywords:

buck converter
simulation model
extended parameters

Available online: https://doi.org/10.26552/com.C.2025.026

ISSN 1335-4205 (print version)
ISSN 2585-7878 (online version)

1 Introduction

The efficient utilization of alternative energy sources is highly relevant in today's energy-intensive era, which has resulted in significant attention being directed toward the field of direct current (DC) power conversion. For this purpose, power semiconductor converters are primarily used, with simulation software considered as one of the most effective development tools in their design [1-6]. The use of integrated switched voltage regulators has greatly simplified the design and construction of the DC power supplies, which are widely utilized, including in transportation. However, a broader range of simulation models for these components is unfortunately lacking. Based on the configuration of such converters, these integrated regulators can be categorized into several groups. The largest group consists of switched regulators designed for step-down (buck) converters, with a manufacturer-recommended connection presented in Figure 1 [7-10].

This configuration includes not only the integrated switched regulator circuit but the additional external components essential for its operation, as well.

2 Regulator model

Based on the key catalog parameters of existing switched voltage regulators, designed for the buck DC-DC converters, a conceptual and universal block diagram can be developed. This diagram is presented in Figure 2.

A universal simulation model of the regulator [11] was developed based on this diagram. This model can be simplified as follows, resulting in a more streamlined, accurate, and efficient design, which subsequently reduces simulation time.

.SUBCKT 2576M Vin On_Off GND FB Vout; Name of subcircuit and parameters
+ PARAMS: Vref=1.23 Imax=3.7 f=52000; Default setting: Vref, Imax, f, Rsw
+ Rsw=0.019 Dmax=0.9 Umax=40 Delay=0u; Dmax, Umax, Delay
VA1 12 60; Ammeter A
V+5 9 GND 5; Power supply + 5V for logical circuits
VG 19 GND DC 0 AC 1 0; Frequency generator with parameters:

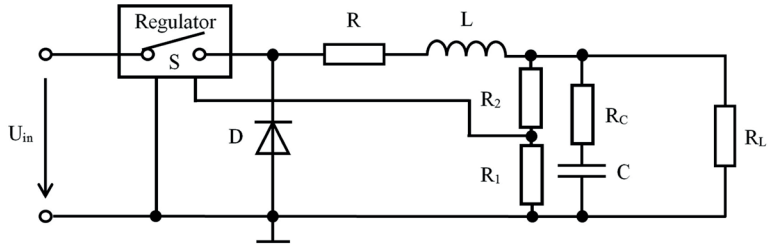

Figure 1 *Configuration of a buck converter with an integrated switched voltage regulator*

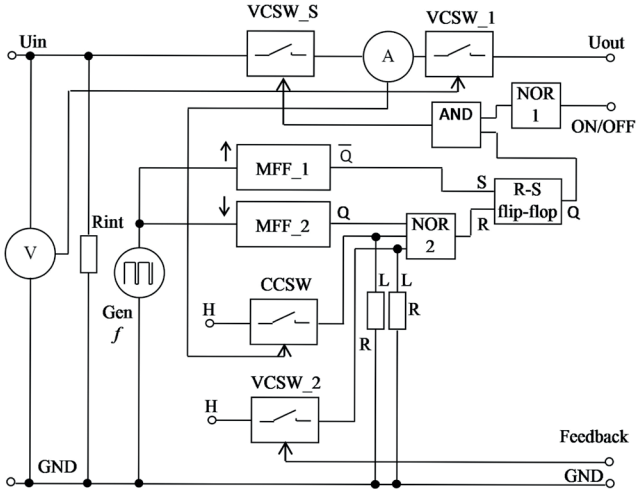

Figure 2 *Block diagram of the proposed universal switched voltage regulator*

+ PWL (0,0) ({Delay} 0); Delay, Dmax, f
+ REPEAT FOREVER (0,0) (10N 5)
+ (+{Dmax/f} 5)(+10N 0)(+10N 0)
+ (+{1/f-Dmax/f} 0) (+10N 0)
+ ENDREPEAT
U7 INV 9 GND On_Off 6 7404 IO_STD; Inverter (INV) (NOR 1)
U5 AND(2) 9 GND 7 6 8 7408 IO_STD; (AND)
SW3 9 10 FB GND SW1; Voltage controlled switch 2 (VCSW_2)
R2 GND 10 390; Resistor R
HCCV+5 11 GND VA1 10; Conversion: switch S current to voltage
SW2 9 13 11 GND SW2; Switch controlled by S current (CCSW)
R1 13 GND 390; Resistor R
SW0 60 Vout Vin GND SW4; Voltage controlled switch 1 (VCSW_1)
SW1 Vin 12 8 GND SW3; Voltage controlled switch S (VCSW_S)
U6 NOR(3) 9 GND 15 13 10 16 7427 IO_STD; (NOR 2)
U4 NAND(2) 9 GND 7 16 17 7400 IO_STD; NAND - part of (R-S flip-flop)
U3 NAND(2) 9 GND 18 17 7 7400 IO_STD; NAND - part of (R-S flip-flop)
XU2 19 19 9 15 20 GND 9 74121; Monostable flip-flop 2 (MFF_2)
XU1 GND GND 19 21 18 GND 9 74121; Monostable flip-flop 1 (MFF_1)

.MODEL SW1 VSWITCH (Ron=0 Roff=1G Von={Vref} Voff={Vref-0.0000001})
.MODEL SW2 VSWITCH (Ron=0 Roff=1G Von={10*Imax} Voff={10*Imax-0.01})
.MODEL SW3 VSWITCH (Ron={Rsw} Roff=1G Von=1.8 Voff=1.79)
.MODEL SW4 VSWITCH (Ron=0 Roff=1000G Von={Umax} Voff={Umax+0.1})
.MODEL 7404 UGATE
.MODEL 7408 UGATE
.MODEL 7427 UGATE
.MODEL 7400 UGATE
.ENDS

.SUBCKT 74121 A1 A2 B Q Q_Neg GND VCC; Subcircuit of monostable flip-flop 74121
U2 INV VCC GND A1 30 7404 IO_STD; Inverter
U3 NAND(2) VCC GND 30 B 29 7400 IO_STD; NAND
U4 JKFF(1) VCC GND; JK flip-flop
+ VCC 27 29 VCC GND 23 24 7476 IO_STD
U5 INV VCC GND 29 28 7404 IO_STD; Inverter
U6 NAND(2) VCC GND 28 23 25 7400 IO_STD; NAND
U7 JKFF(1) VCC GND; JK flip-flop
+ 23 31 25 GND VCC 27 26 7476 IO_STD
U8 INV VCC GND 24 Q 7404 IO_STD; Inverter
U9 INV VCC GND 23 Q_Neg 7404 IO_STD; Inverter
.MODEL 7476 UEFF
.ENDS

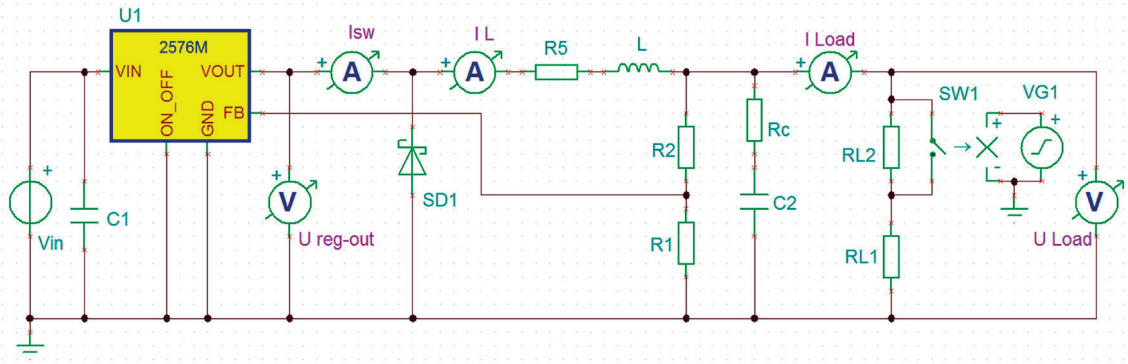

Figure 3 *Circuit diagram of the configuration under investigation in the TINA program*

The accuracy and functionality of the LM2576-ADJ regulator model can be validated by incorporating it into a buck converter circuit with a dynamically variable resistive load, configured with the following parameters: L = 100 µH, R5 = 200 mΩ, Vin = 40 V, R1 = 2 kΩ, R2 = 22.39 kΩ, C1 = 100 µF, C2 = 1 mF, Rc = 40 mΩ, RL1 = 5 Ω, RL2 = 32.5 Ω, as shown in Figure 3. The diode SD1 was selected as the MBR360.

For the simulation, the TINA software (Toolkit for Interactive Network Analysis) [12] was employed. This program is fully compatible with the globally recognized PSPICE software, including its libraries and operational rules [13].

A comparison of the results obtained through simulation to those reported in the datasheets, both under constant load and with a step change in load, is presented in Figure 4.

A correlation of the waveforms clearly demonstrates that the model accurately approximates the behavior of the real component in both static and dynamic operating modes.

The advantages of using the proposed simulation model for the switched voltage regulator can be illustrated through a comparison to existing models, although such models are relatively few in number. The most widely used model is the LM2576ADJ simulation model, available on the Texas Instruments website [14]. In terms of model simplicity, its description spans 125 lines, whereas the newly proposed model is described in only 38 lines. Regarding computation speed, this is, of course, dependent on the hardware of the computer used and the settings of the simulation software. Therefore, analyzing the absolute time savings is not meaningful. However, a relative analysis is possible. Specifically, a simulation analysis of the circuit shown in Figure 3 was performed on the same machine, using the same software, and under identical conditions. The comparison of computation times revealed that the use of the newly proposed model resulted in calculation times that were half of those of the analysis employing the LM2576ADJ model from the Texas Instruments website.

The limitations of the proposed simulation model lie in its inability to include the thermal conditions of the voltage regulator in the circuit analysis, as well as in the fact that the user is constrained by the properties of the individual simulation elements used in constructing the switched regulator model. These limitations, however, are general constraints inherent to the use of PSPICE simulation software, which restricts its application in any electrical circuit simulation. The same holds true for the impact of component parameter tolerances on the model's performance.

This validation of the model enables its application in designing circuits that extend the output parameters of a buck converter beyond its catalog specifications. Additionally, it leverages the significant advantages of the regulator in the form of an integrated circuit, including its relatively low cost, wide availability, and high level of integration, which incorporates control, regulation, and protection circuits for the converter.

3 Increase in the output current of a buck converter with a switched voltage regulator

The first option involves the parallel arrangement of separate converters with regulators. The current division between the regulators is inversely proportional to the ratio of their inductances, meaning that a higher inductance results in a lower current for the corresponding converter. When identical regulators are used in both converters connected in parallel, selecting the same inductance values is advantageous, as it ensures even current distribution. Additionally, it is beneficial to use a single common diode (SD1), two separate summing diodes (SD2 and SD3), and a shared feedback control (FB). To obtain simulation results, the LM2576 switched regulator model will be employed. Due to the limitations of the simulation (since the oscillators of the individual real controllers are not time-synchronized), the time course of controller U1 is shifted by 10 µs relative to controller U2. The wiring diagram of the simulated circuit is presented in Figure 5.

The circuit parameters are as follows: L1 = L2 = 100 µH, R3 = R5 = 460 mΩ, Vin = 40 V, R1 = 1 kΩ, R2 = 6.12 kΩ, C1 = 100 µF, C2 = 1 mF, Rc = 181 mΩ. Diodes SD1, SD2, and SD3 were selected as MBR360.

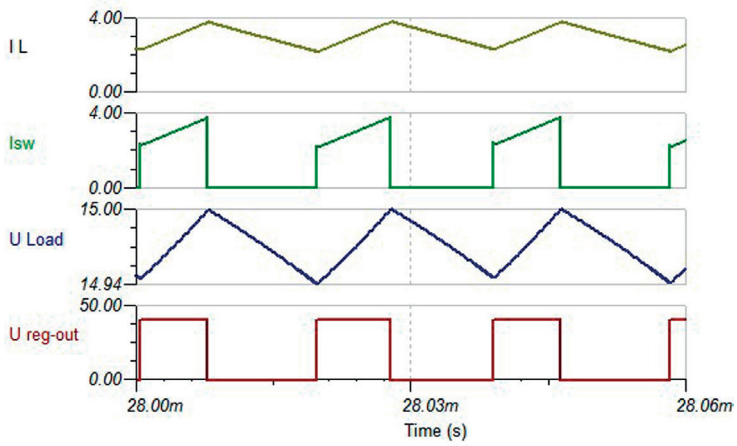

a)

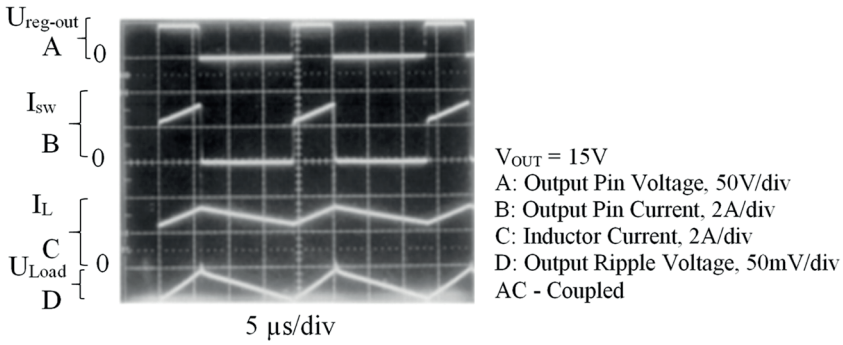

b)

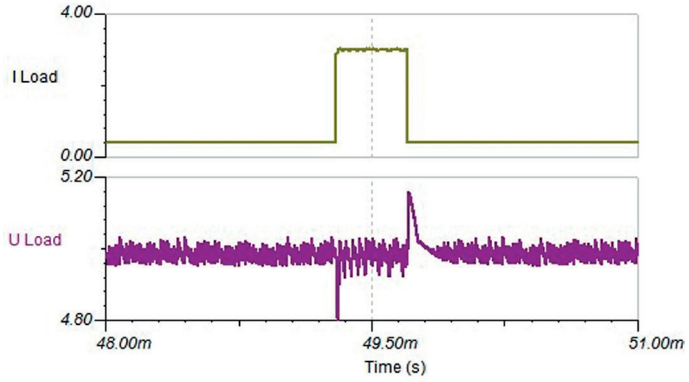

c)

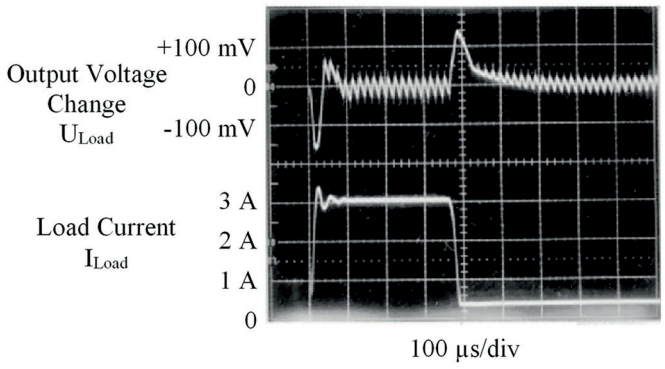

d)

Figure 4 *Key parameters of the converter: a) static results obtained through simulation at constant load; b) results from the manufacturer's datasheet for the LM2576-ADJ at constant load; c) results obtained through simulation during the step change in load; d) results from the manufacturer's datasheet for the LM2576-ADJ during the step change in load*

The load resistors have values of RL_1 = 1 Ω and RL_1 = 1.5 Ω. The main waveforms of the investigated circuit, obtained through simulation, are shown in Figure 6.

The results obtained from the measurements are presented in Figure 7.

The second method for increasing the output current of the buck converter is to incorporate a bipolar transistor (BT) into the circuit, as shown in Figure 8.

The total maximum allowable current of the converter is given by the following expression:

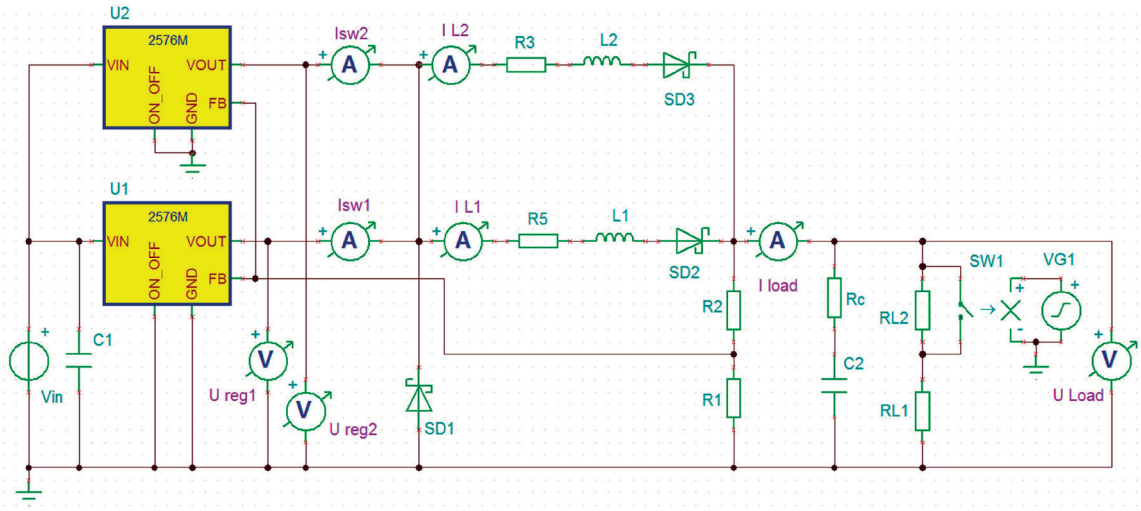

Figure 5 *Simulated parallel configuration of converters with separate regulators under a step change in load*

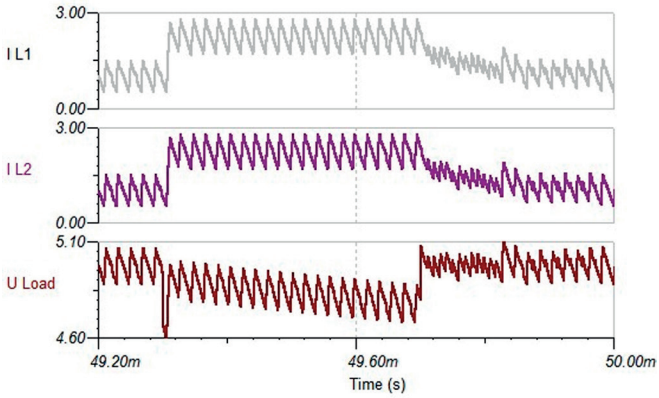

Figure 6 *Main waveforms of the parallel connection of converters with separate regulators under a step change in load, obtained through simulation in the TINA program*

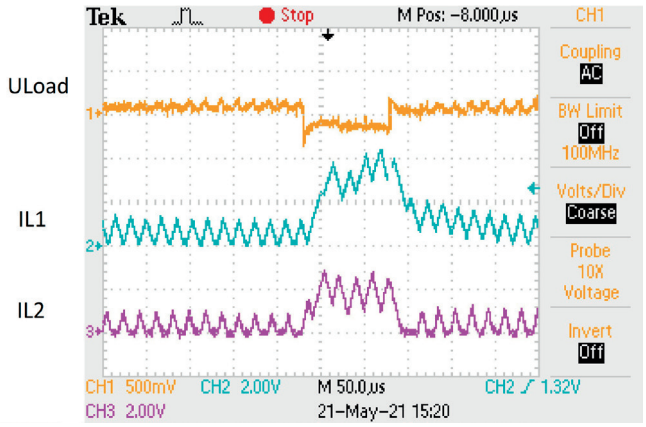

Figure 7 *Measured waveforms of the parallel-connected converters with separate regulators under a step change in load (current scale: 1 V = 1 A)*

$$I_{cmax} = (1 + h_{21E})I_{max}\,, \tag{1}$$

where:
I_{max} is the maximum allowable current of the regulator used,
h_{21E} is the current gain of the bipolar transistor.

The circuit parameters are as follows: L = 100 µH, R3 = 460 mΩ, Vin = 40 V, R1 = 1 kΩ, R2 = 6.12 kΩ, C1 = 100 µF, C2 = 1 mF, Rc = 181 mΩ. The SD1 diode used is of the MBR360 type. The load resistors have values of RL1 = 0.6 Ω and RL2 = 2 Ω. The results obtained from simulating the circuit are shown in Figure 9, while the

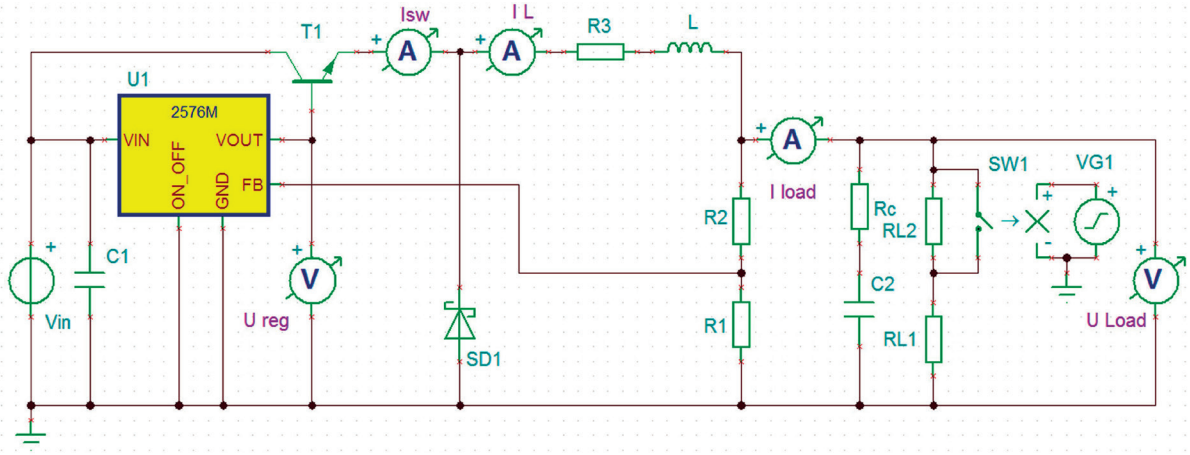

Figure 8 *Wiring diagram of the switching regulator with output current extension using a bipolar junction transistor*

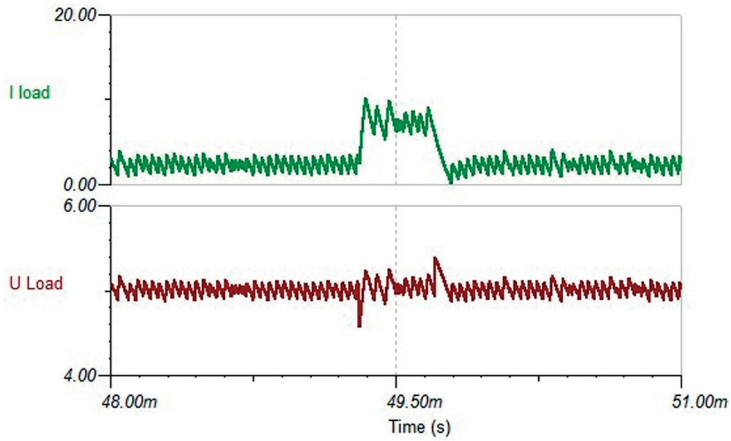

Figure 9 *Voltage and load current waveforms of the switched voltage regulator using a bipolar transistor during a step change in load, obtained through simulation in the TINA program*

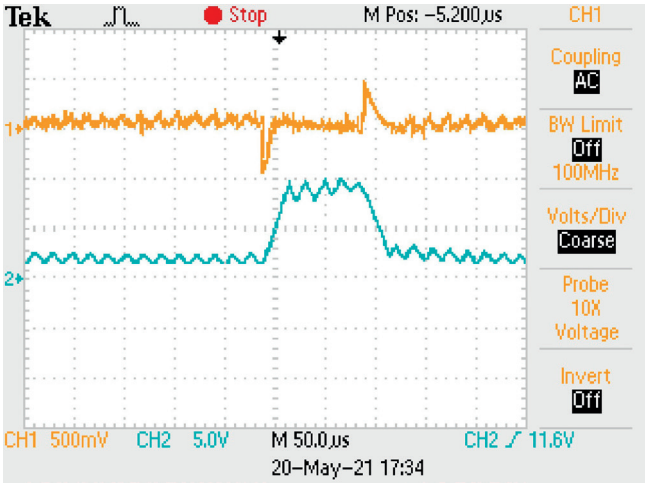

Figure 10 *Voltage and load current (blue) of the switched voltage regulator using a bipolar transistor during a step change in load, obtained through measurement (current scale: 1 V = 1 A)*

verification results, obtained from measurements on a laboratory sample of the transducer, are presented in Figure 10.

Based on the aforementioned considerations, it can be concluded that both analyzed solutions are practically applicable when an increased output current from the converter is required. In terms of output voltage regulation, the more effective, though costlier, option involves using multiple regulators connected in parallel. The simpler alternative, which employs a switching bipolar transistor (BT), is less expensive but offers lower output voltage regulation quality. Additionally, due to the switching speed of the BT, this solution is suitable only for regulators with lower switching frequencies.

4 Increase in the output voltage of a buck converter using the switched voltage regulator

To demonstrate a potential increase in the voltage and current output parameters of a switched voltage regulator, the LM2574 regulator type [10] was chosen. Its advantages include affordability, compact size, integrated current limiting, and a built-in voltage regulator. However, its limitations include a maximum current of 0.5 A and a voltage limit of 40 V. These limitations can be overcome by employing the circuit shown in Figure 11 [15].

The connection is based on the integrated circuit (IC) LM2574, which generates the control pulses for the converter based on the output voltage, obtained from the resistive divider R2 and R1. This voltage is compared with the reference voltage U_{ref} = 1.23 V. According to the datasheet, the resistance value of R1 should range from 1 kΩ to 5 kΩ. The required output voltage is set by potentiometer R2, as described by:

$$R_2 = R_1\left(\frac{U_{out}}{U_{ref}} - 1\right). \tag{2}$$

The reduced supply voltage for the regulator and the isolated DC-DC converter (TRACO) is achieved using a Zener stabilizer, implemented with components R13, Z2, and C3. A similar stabilizer, formed by elements R6, Z3, and C4, generates a 5V supply for the output side of the optical isolator 6N137, whose input LED is driven by the output signal VOUT from the LM2574. Since the optocoupler inverts the signal, it must be inverted again and amplified using transistor T5. The resulting control signal is impedance-matched by the complementary transistor pair T2 and T4 and passed through resistor R12 to the gate of the power switching transistor MOSFET (or IGBT) T1, which is dimensioned for the required higher voltage and current. Current limitation in the circuit is achieved using the sensing diode D1, where the voltage across it in the closed state corresponds to the current flowing through the switch. This voltage triggers the opening of transistor T3, generating a signal that corresponds to the current magnitude on the resistor divider R7 and R14. This signal is then connected to the ON/OFF control input of the LM2574 regulator, which is switched off when the voltage exceeds the threshold value of 1.4 V, as specified in the datasheet. The allowable current of transistor T1 can be adjusted using trimmer R5, thereby ensuring current limitation for the entire converter.

It is also important to note that DC-DC converters can operate in two modes:

- CCM (Continuous Conduction Mode): The current i_{L3} supplied by the inductor to the load when the switch S is open is always greater than zero.

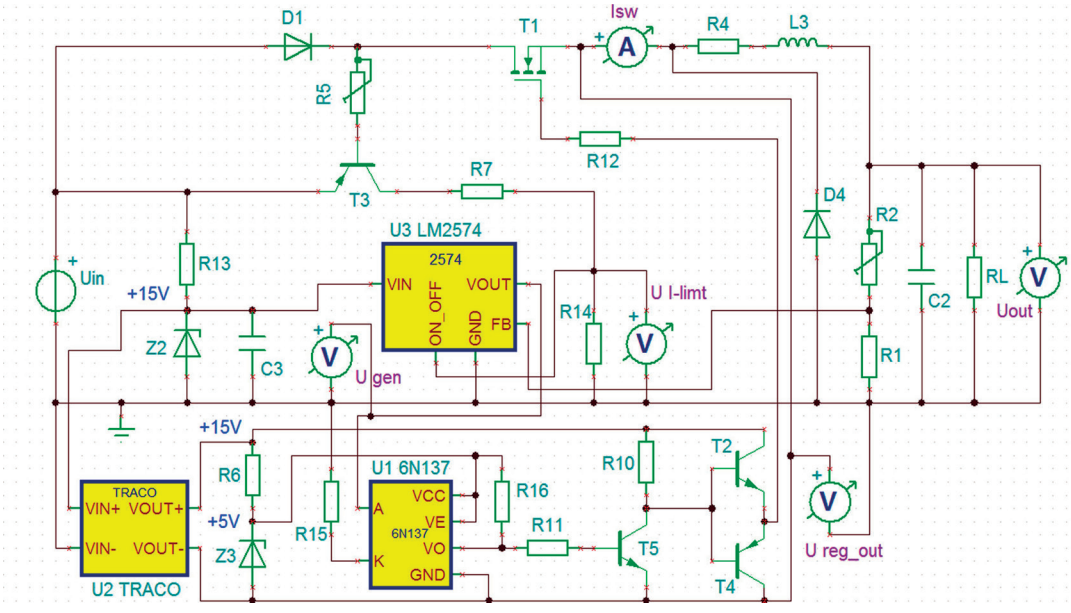

Figure 11 *Configuration of a buck DC-DC converter with the LM2574-ADJ, extending its current and voltage limits*

- DCM (Discontinuous Conduction Mode): The current i_{L3} is zero at certain points during the switching period.

The mode in which the converter operates primarily depends on the inductance value L of the inductor L3, the duty cycle D, and the switching frequency f. The inductance value that defines the boundary between CCM and DCM is given by the following relation for a buck DC-DC converter [16]:

$$L_b = \frac{(1-D)R_L}{2f}. \tag{3}$$

For L > L_b, the converter operates in Continuous Conduction Mode (CCM). Based on the operational

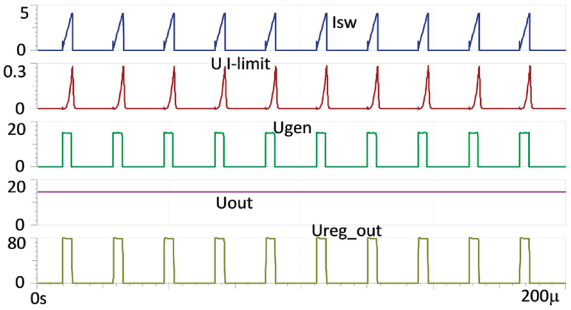

a)

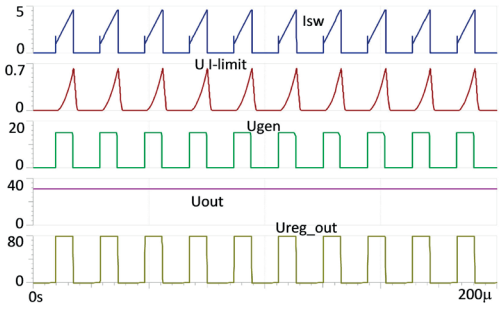

b)

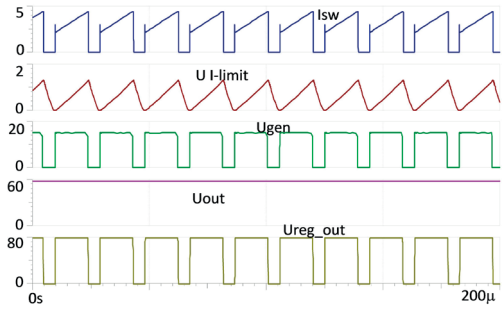

c)

Figure 12 *Converter waveforms obtained from the simulation in the TINA program: a) Uout=14.3 V, b) Uout=31 V, c) Uout=58 V*

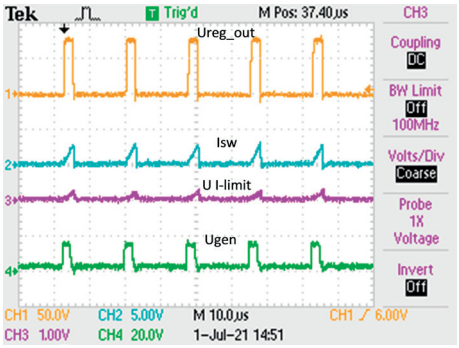

a)

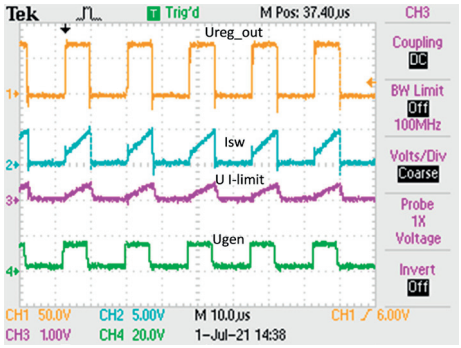

b)

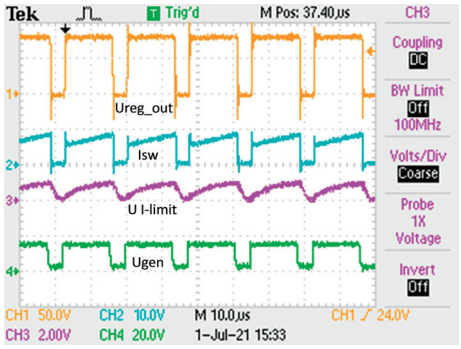

c)

Figure 13 *Converter waveforms obtained through measurement: a) Uout=14.3 V, b) Uout=31 V, c) Uout=58 V*

principle of the regulator, it is evident that when using a switched voltage regulator, the duty cycle (D) varies, which in turn alters the mode of operation of the converter, transitioning between CCM and Discontinuous Conduction Mode (DCM). The current i_C flowing through the capacitor C2 induces a small ripple in the output voltage U_{out}. To limit this ripple to the desired value U_{ripple}, the capacitance of capacitor C2 must meet a minimum value, as given by [16]:

$$C_{\min} = \frac{(1-D)U_{out}}{8U_{ripple}Lf^2}. \quad (4)$$

The waveforms obtained from the simulation in the TINA program for three different output voltage values are shown in Figure 12. The corresponding measurement results from the converter circuit are presented in Figure 13. The key component values of the converter are as follows: Uin = 80 V, f = 52 kHz, R1 = 1 kΩ, R2 = 10.62 kΩ (24.2 kΩ, 46.15 kΩ), R4 = 360 mΩ , L3 = 330 µH, C2 = 470 µF, RL = 11 Ω. The maximum inverter switching current has been set to 8 A.

The measured output voltage-current (V-I) characteristics of the converter, for the output voltages Uout = 14.3 V, Uout = 31 V and Uout = 58 V, are shown in Figure 14.

An example of the laboratory implementation of the described converter is shown in Figure 15. A comparison of the results obtained from both simulation and measurement demonstrates good agreement in the waveforms, highlighting the practical applicability of the proposed configuration. Utilizing the cost-effective LM2574 circuit, along with the addition of several other components, it is relatively straightforward to configure a buck DC-DC converter capable of delivering power in the hundreds of watts, with an output voltage that can reach several hundred volts.

5 Recommendations for enhancing the EMC of a buck DC-DC converter

An important consideration in the design of a buck converter is electromagnetic compatibility [17]. From this perspective, the most critical component is the inductance L, implemented as a technical coil, which serves as a source of electromagnetic emissions. These emissions can significantly affect the operation of nearby electrical and electronic equipment. The critical nature of this component arises not only from the relatively high switching frequencies but, more importantly, from the high switching currents. This issue is clearly illustrated in Figure 16, which shows the magnetic field generated by both a toroidal and a cylindrical coil when subjected to a harmonic current with an amplitude of 10 A and a frequency of f = 52 kHz.

The results of the magnetic field distribution were

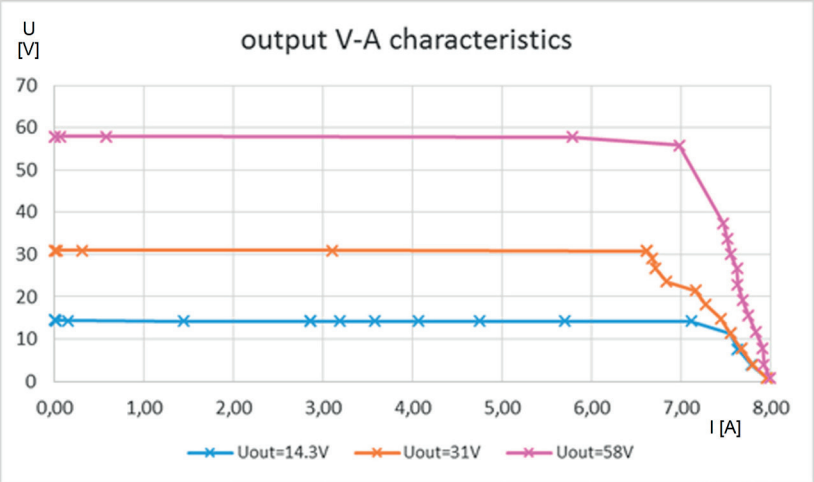

Figure 14 *Measured output voltage-current (V-I) characteristics of the converter*

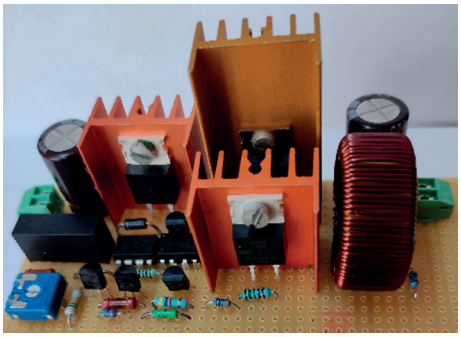

Figure 15 *Demonstration of the laboratory prototype of the converter*

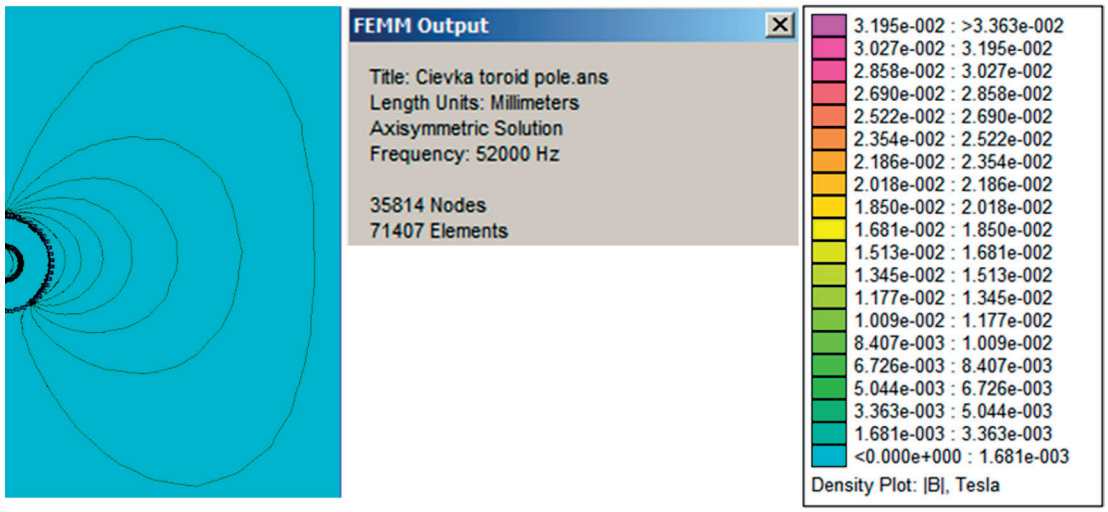

a)

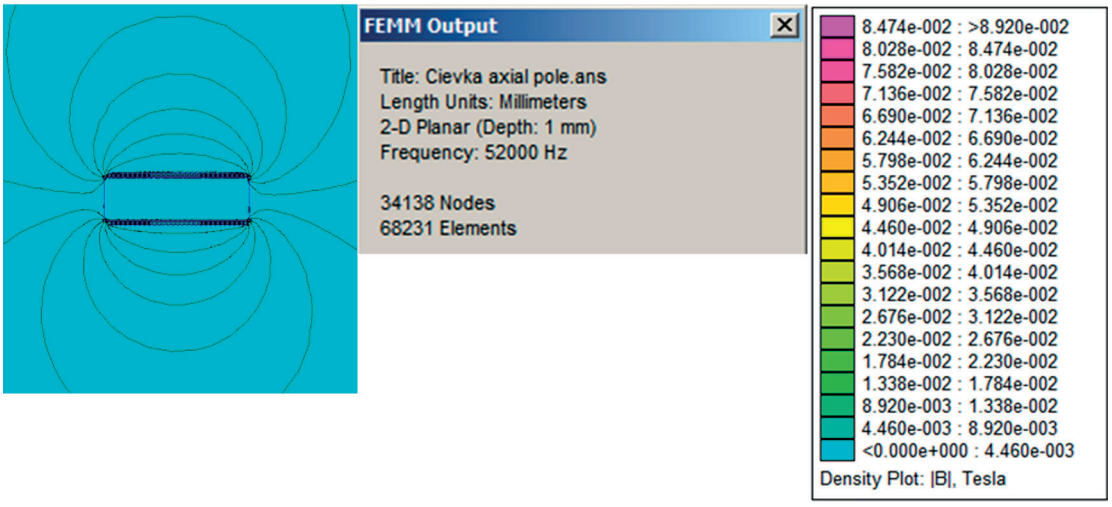

b)

Figure 16 *Radiated magnetic field of the coil: a) toroidal, b) axial*

obtained using the FEMM simulation program [18], which utilizes the finite element method. To mitigate the radiation, it is sufficient to shield the coil with 0.3 mm thick aluminum foil [19]. This solution is illustrated in Figure 17.

The simulations demonstrate that substantial improvements in the electromagnetic compatibility of the buck DC-DC converters can be achieved by shielding the technical coil with 0.3 mm-thick aluminum foil.

6 Conclusion

By comparing Figures 4a) and 4b), an overview of the accuracy of the static parameters in the converter, using the improved and simplified regulator model, is obtained, showing an agreement of 95%. Similarly, the accuracy of the dynamic parameters is assessed through Figures 4c) and 4d), where the results demonstrate approximately 93% agreement. This is an excellent outcome, particularly considering that accuracy is influenced not only by the regulator model but by the realism of the models for the external components (MOSFET, diode), as well.

The presented universal model of the switching voltage regulator is based on the equivalence of its typical properties, which significantly simplifies the model. Unlike existing regulator models, it allows for easy modification of individual parameters, providing a more accurate reflection of the characteristics of the actual components used, particularly when components are employed multiple times in a single configuration.

Using this model, recommended configurations of switching regulators were tested to enhance the output power of a buck DC-DC converter. These configurations included parallel regulator connections, the addition of a switching bipolar transistor, and the use of external MOSFET or IGBT transistors. The results obtained from measurements conducted on laboratory samples of the converters demonstrate their practical applicability, offering low costs and compact

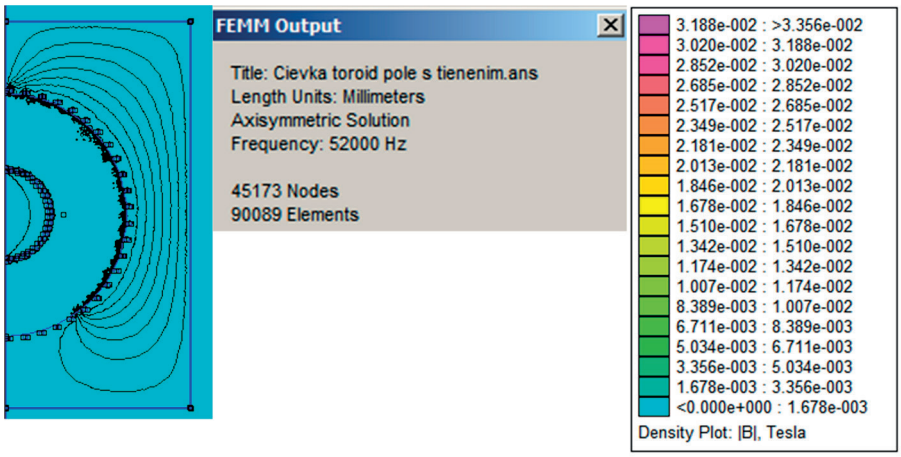

a)

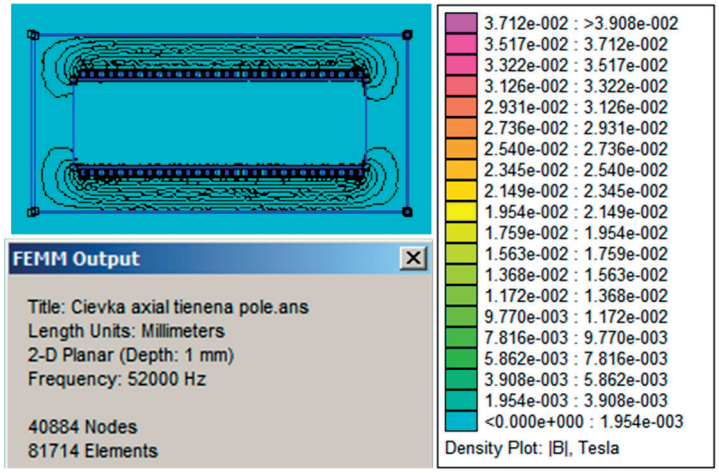

b)

Figure 17 *Radiated magnetic field of an aluminum-shielded coil to a thickness of 0.3 mm: a) toroidal, b) axial*

dimensions. The improvement of the converter's output parameters is fundamentally determined by the limiting characteristics of the external components connected to the regulator. In the case of increasing the output current through the parallel connection of switched regulators, the limiting factor is primarily the number of regulators, particularly in terms of spatial arrangement. When increasing the output current by adding a bipolar transistor circuit, the limitations are imposed by the maximum output current of the integrated regulator, the current amplification factor of the bipolar transistor, and, ultimately, its frequency characteristics, which must be compatible with the frequency of the integrated regulator. However, it is important to note that even in this configuration, the converters can be further connected in parallel if additional current increase is needed. For increasing the output voltage of the converter, the proposed configuration is constrained by the maximum allowable drain-source voltage (u_{DS}) of the used MOSFET transistor, its frequency parameters (which must match the integrated regulator's frequency characteristics), and the power losses in the Zener stabilizer circuit or the TRACO converter, which are used to generate the low-voltage supply for the switched regulator and additional logic circuits.

A significant contribution of this study is the simulation evidence demonstrating a substantial improvement in the electromagnetic compatibility (EMC) of the constructed converters. This improvement was achieved through the straightforward application of shielding foil around the primary source of radiation - the technical coil.

Acknowledgment

The authors received no financial support for the research, authorship and/or publication of this article.

Conflicts of interest

The authors declare that they have no known competing financial interests or personal relationships that could have appeared to influence the work reported in this paper.

References

[1] BERES, M., KOVAC, D., VINCE, T., KOVACOVA, I., MOLNAR, J., TOMCIKOVA, I., DZIAK, J., JACKO, P., FECKO, B., GANS, S. Efficiency enhancement of non-isolated DC-DC interleaved buck converter for renewable energy sources. *Energies* [online]. 2021, **14**(14), 4127. eISSN 1996-1073. Available from: https://doi.org/10.3390/en14144127

[2] WANG, L., ZHANG, D., DUAN, J., GU, R. Research on high-performance multiphase DC-DC converter applied to distributed electric propulsion aircraft. *IEEE Transactions on Transportation Electrification* [online]. 2023, **9**(3), p. 3545-3563. EISSN 2332-7782. Available from: https://doi.org/10.1109/TTE.2022.3207142

[3] YAMA, O., KHYZHNIAK, T., BONDARENKO, O. Analysis of modified non-isolated DC-DC converters and solutions to improve their characteristics. In: IEEE 4th KhPI Week on Advanced Technology: proceedings [online]. 2023. eISBN 979-8-3503-9553-2, p. 1-6. Available from: https://doi.org/10.1109/KhPIWeek61412.2023.10312965

[4] FRIVALDSKY, M., PCOLA, M., BIEL, Z., KUCERA, R., FRANKO, M., HOLCEK, R. Node ringing reduction of synchronous buck converter. *Communications - Scientific Letters of the University of Zilina* [online]. 2023, **25**(3), p. C48-C55. ISSN 1335-4205, eISSN 2585-7878. Available from: https://doi.org/10.26552/com.C.2023.054

[5] LYU, Y., SANUSI, B. N., OUYANG, Z. Modeling and analysis of coupling effect in four legged core for multi-phase buck converter. In: IEEE Applied Power Electronics Conference and Exposition: proceedings [online]. 2023. eISBN 978-1-6654-7539-6, eISSN 2470-6647, p. 3307-3313. Available from: https://doi.org/10.1109/APEC43580.2023.10131131

[6] SIMCAK, J., FRIVALDSKY, M., RESUTIK, P. The power analysis of semiconductor devices in multi-phase traction inverter topologies applicable in the automotive industry. *Communications - Scientific Letters of the University of Zilina* [online]. 2024, **26**(3), p. C21-C38. ISSN 1335-4205, eISSN 2585-7878. Available from: https://doi.org/10.26552/com.C.2024.034

[7] MOBAYEN, S., BAYAT, F., LAI, CH.-CH., TAHERI, A., FEKIH, A. Adaptive global sliding mode controller design for perturbed DC-DC buck converters. *Energies* [online]. 2021, **14**(14), 1249.e ISSN 1996-1073. Available from: https://doi.org/10.3390/en14051249

[8] Datasheet LM2576 - Texas Instruments [online] [accessed 2024-10-18]. Available from: https://www.ti.com/lit/ds/symlink/lm2576.pdf?ts=1626045022539&ref_url=https%253A%252F%252Fwww.google.com%252F

[9] Design tools and simulation - Texas Instruments [online] [accessed 2024-10-11]. Available from: https://www.ti.com/product/LM2576

[10] Datasheet LM2574 - Texas Instruments [online] [accessed 2024-10-18]. Available from: https://www.ti.com/lit/ds/snvs104f/snvs104f.pdf?ts=1626064117944&ref_url=https%253A%252F%252Fwww.google.com%252F

[11] KOVAC, D., VINCE, T., BERES, M., MOLNAR, J., DZIAK, J., JACKO, P., KOVACOVA, I. A universal PSpice simulation model of a switched buck voltage regulator. *Energies* [online]. 2022, **15**(15), 8209. eISSN 1996-1073. Available from: https://doi.org/10.3390/en15218209

[12] TINA-TI SPICE-based analog simulation program - Texas Instruments [online] [accessed 2024-10-21]. Available from: https://www.ti.com/tool/TINA-TI

[13] PSpice reference guide [online] [accessed 2024-10-21]. Available from: https://www.seas.upenn.edu/~jan/spice/PSpice_ReferenceguideOrCAD.pdf

[14] LM2576 unencrypted PSpice transient model - Texas Instruments [online] [accessed 2024-10-21]. Available from: https://www.ti.com/product/LM2576#design-development

[15] KOVAC, D., KOVACOVA, I., SCHWEINER, D. Wiring for extending the current and voltage load capacity of a switched voltage regulator [online]. Slovak patent No. 289249. Industrial Property Office of the SR, 2024. Available from: https://wbr.indprop.gov.sk/WebRegistre/Patent/Detail/129-2019?csrt=9841336417737460554

[16] RASHID, M. H. *Power electronics handbook*. 3. ed. Elsevier Inc., 2011. ISBN 978-0-12-382036-5.

[17] KOVACOVA, I., KOVAC, D. Electromagnetic coupling - EMC of electrical systems. *Journal on Communications Antenna and Propagation* [online]. 2014, **4**(2), p. 51-57. ISSN 2039-5086, eISSN 2533-2929. Available from: https://www.praiseworthyprize.org/jsm/index.php?journal=irecap&page=article&op=view&path%5B%5D=0103

[18] FEMM application [online] [accessed 2024-10-07]. Available online: https://www.femm.info/wiki/HomePage

[19] KUBIK, Z., SKALA, J. Shielding effectiveness simulation of small perforated shielding enclosures using FEM. *Energies* [online]. 2016, **9**(3), p.1-12. eISSN 1996-1073. Available from: https://doi.org/10.3390/en9030129